Directed diffusion of reconstituting dimers

2007 J. Phys.: Condens. Matter 19 065112

(http://iopscience.iop.org/0953-8984/19/6/065112)

INSTITUTE OF PHYSICS PUBLISHING JOURNAL OF PHYSICS: CONDENSED MATTER

J. Phys.: Condens. Matter **19** (2007) 065112 (12pp) doi:10.1088/0953-8984/19/6/065112

Directed diffusion of reconstituting dimers

Mustansir Barma[1,2], **Marcelo D Grynberg**[3] **and Robin B Stinchcombe**[2,4]

[1] Department of Theoretical Physics, Tata Institute of Fundamental Research, Mumbai 400005, India
[2] Isaac Newton Institute for Mathematical Sciences, 20 Clarkson Road, Cambridge CB3 0EH, UK
[3] Departamento de Física, Universidad Nacional de La Plata, (1900) La Plata, Argentina
[4] Rudolf Peierls Centre for Theoretical Physics, University of Oxford, 1 Keble Road, Oxford OX1 3NP, UK

Received 1 September 2006, in final form 10 October 2006
Published 22 January 2007
Online at stacks.iop.org/JPhysCM/19/065112

Abstract

We discuss the dynamical aspects of an asymmetric version of assisted diffusion of hard core particles on a ring studied by Menon *et al* (1997 *J. Stat. Phys.* **86** 1237). The asymmetry brings in phenomena like kinematic waves and effects of the Kardar–Parisi–Zhang non-linearity, which combine with the feature of strongly broken ergodicity, a characteristic of the model. A central role is played by a single non-local invariant, the irreducible string, whose interplay with the driven motion of reconstituting dimers, arising from the assisted hopping, determines the asymptotic dynamics and scaling regimes. These are investigated both analytically and numerically through sector-dependent mappings to the asymmetric simple exclusion process.

1. Introduction

The issue of universality classes in non-equilibrium statistical systems is often linked to the existence of conservation laws [1]. Normally, the number of conservation laws is finite, leading to the occurrence of dynamically disjoint sectors whose number grows as a power of the system size. However, certain dynamical processes involving composite objects exhibit strongly broken ergodicity, with the number of disjoint sectors growing exponentially with system size, as a result of having an extensive number of conservation laws. Examples studied earlier include deposition and evaporation ($\bullet\bullet\bullet \leftrightarrow \circ\circ\circ$) [2–5], and diffusion ($\bullet\bullet\circ \leftrightarrow \circ\bullet\bullet$) [6] of bunches of particles. If these moves are interpreted as involving trimers or dimers (in general k-mers), then the k-mers in question do not keep their identity and can reconstitute in time. The dynamical moves in these models do not connect configurations in different sectors, implying that the steady state is not unique and depends strongly on the initial condition. Moreover, the form of the long-time decay of time-dependent correlations in the steady state varies strongly from one sector to another. In one dimension, both the partitioning of phase space into many sectors and the accompanying dynamical diversity could be understood in terms of a non-local construct known as the irreducible string (IS) which is an invariant of the motion. The IS provided a convenient label for each sector [4]. Moreover, the position of the elements of the

IS was the relevant 'slow' variable in the problem, and thus governed the long-time dynamics in different sectors. The dynamical diversity found in different sectors (ranging from different power law decays to stretched exponentials) could be accounted for in terms of the differences in the IS from sector to sector [5]. In turn, the IS can be used to construct an extensive number of conservation laws, although it turns out that these involve non-local combinations of the site occupancies [4].

All such studies known to us involve a symmetric movement of the IS. Here we study the dynamical consequences of an asymmetric (directed) motion of the IS. This brings in new phenomena associated with driven diffusive systems, such as kinematic waves and effects of the Kardar–Parisi–Zhang (KPZ)/Burgers non-linearity, present in the 1-D asymmetric simple exclusion process (ASEP) [7, 8]. We investigate these effects by studying the directed diffusion of reconstituting dimers (DDRD). The model resembles the diffusing reconstituting dimer model studied in [6], the only difference being that we allow for only forward motion of the dimers ($\bullet\bullet\circ \rightarrow \circ\bullet\bullet$), in contrast to the two-way motion studied in that paper. The construction of the IS is the same for symmetric/asymmetric motion, but the dynamics of dimers (and of the IS) is quite different in the directed case.

It turns out that there is a correspondence between the DDRD and the well-studied ASEP, though of a generalized sort, leading to extra features including additional wheeling motion of sites, oscillations of correlation functions and other new kinetic effects. These typically result from the combination of collective driving and the invariant, but moving, IS. Interestingly, there is a very useful correspondence between the DDRD and a three-species exclusion process. Further, the problem of forward-moving non-reconstituting (hard) dimers which keep their identity is recovered in the DDRD, in a particular sector.

As in the previous studies of dynamic diversity, Monte Carlo (MC) simulation is a key ingredient in trying to understand the dynamics. In particular we study time-dependent correlation functions in different sectors and use analytic reductions related to the specific form of the IS and the motion of its elements to correlate the diverse behaviour seen in the simulations with properties of the ASEP. Remarkably close correspondences in non-universal as well as scaling properties are seen.

The development begins (section 2) with an introduction to the model and then moves on in the same section to the following sequence of emerging topics: equivalence to the three-species process and correspondences with the ASEP, whose properties are summarized. In section 3 we study the kinetics within a particularly simple sector in which the problem is tantamount to that of non-reconstituting dimers. New effects such as wheeling of sites in the equivalent ASEP, resulting from the combination of driving and the composition of dimers, are shown to have important consequences for autocorrelation functions. These show early oscillations and later a decay, whose form (exponential or power law), is decided by a critical condition related to wheeling and kinematic wave velocities. The long-time behaviour shows scaling, and universality in the sense of data collapse to ASEP scaling functions, but with sector-specific parameters. The theoretical and MC results are extended to more general sectors in section 4, via investigations of sublattice currents, sublattice current–density relations and consequent kinematic wave velocities. Section 5 is mainly concerned with spatial correlations in a particular sector, involving MC results and their exact analysis via one of the equivalent models. Section 6 contains a concluding discussion.

2. DDRD model and correspondence to ASEP

The DDRD model consists of a ring of L sites, each of which may be singly occupied (occupation variable $n_i = 1$) or empty ($n_i = 0$). Any of the 2^L possible configurations is

then an L-bit binary string. The system evolves stochastically through the move $110 \to 011$, which represents the directed diffusion (rightward hopping) of reconstituting dimers (DDRD). This is equivalent to stochastic hopping of holes two steps to the left (i.e. staying on the same sublattice) provided the intervening site is occupied. The process is the totally asymmetric alternative to the fully symmetric reconstituting dimer diffusion process (DRD) [6] which is known to be strongly non-ergodic due to the existence of a conserved string of variables, the IS. All states linked by the dynamic process have the same IS, so the phase space divides into many sectors, $\sim\lambda^L$ in number, where λ is the Golden number $(\sqrt{5}+1)/2$. All these properties are shared by the asymmetric generalizations. The IS for a given sector can be obtained from any state in the sector by deleting from its L-bit string any pair of adjacent 1s and repeating the procedure until no more deletions are possible (the result is independent of the order of deletion). For instance, the configuration $\mathcal{C} \equiv 11101001111010$ leads to the IS 10100010.

An equivalent representation of configurations, of the IS and of the process, uses characters A, B, C related to the binary variables by $A = 11, B = 10, C = 0$ [6]. With the periodic boundary conditions used here any DDRD configuration can be uniquely decomposed into a configuration of As, Bs and Cs. For example, the configuration $\mathcal{C}$ of the last paragraph can be written as $ABBCAACB$. Moreover, the totally asymmetric dimer hopping move $110 \to 011$ corresponds to either $AB \to BA$, or $AC \to CA$; the former move involves dimer reconstitution. The IS construction now corresponds to deletion of all As, so the IS is a string of only Bs and Cs, e.g. for the configuration $\mathcal{C}$ defined above the IS is $BBCCB$. The absence of any exchange of Bs and Cs in the DDRD process verifies the conservation of the IS.

In terms of the characters A, B, C, the DDRD process has an obvious and important analogy with the (totally) asymmetric exclusion process (ASEP), in which mutually excluding particles hop to nearest neighbour vacancies on the right. In this correspondence the dimers A play the role of the ASEP particle, and the Bs and Cs of the IS correspond to ASEP vacancies. In order to exploit the correspondence here and later, we use N_A, N_B, N_C to denote the numbers of dimers, 10 pairs and single zeros, respectively. Then the lengths of the DDRD lattice, the IS, and the ASEP lattice are $L = 2N_A + 2N_B + N_C$, $\mathcal{L} = 2N_B + N_C$, and $L_X = N_A + N_B + N_C$, respectively.

The particle density in the ASEP is $x = N_A/L_X$, and the fraction of zeros of C type is $y = N_C/(N_B + N_C)$. Then, in the case of a periodic IS, if the periodic unit $[\cdots]$ of the IS contains n_B Bs and n_C Cs, we have $y = n_C/(n_B + n_C)$. It is straightforward to show from these definitions that $L/L_X = 2 - y(1 - x)$. This ratio provides a metric factor particularly important for converting known currents, tagged hole velocities and particle densities for the ASEP into corresponding DDRD quantities. An important point is that the ASEP image of a fixed DDRD site is not fixed but moves forward and wheels around the periodic ring. The causes and consequences of wheeling are discussed in detail in section 3.

We conclude the section by recalling some facts about the ASEP that we will need later. On a ring, the ASEP has a product-measure uniform steady state (SS), with current $J_X = x(1-x)$ at ASEP particle density x. Density fluctuations move as a kinematic wave through the system [8, 9], with velocity $U = \partial_x J_X = (1 - 2x)$. Also, in the long-time scaling regime, the ASEP density–density correlation function $C_X(r, t) \equiv \langle n(r, t)n(0, 0)\rangle - \langle n\rangle^2$ is of the form

$$C_X(r, t) \propto t^{-2/3} g''(s), \qquad s = \tfrac{1}{2}(J_X t^2)^{-1/3}(r - Ut). \tag{1}$$

It is known (equation (4.8) of [12]) that in the limit of large s, $g''(s) \sim \exp(-\mu|s|^3)$ with $\mu \simeq -0.295$, so the correlation function is exponentially decaying in time at large time t. The exception is when the co-moving condition $r = Ut$ applies, a special case being the autocorrelation function ($r = 0$) when $x = 1/2$ (making $U = 0$). In these cases the correlation function shows $t^{-2/3}$ power law decay in time.

In view of the DDRD–ASEP correspondence, one might expect similar behaviour for asymmetrically diffusing dimers, unlike the symmetrically diffusing dimers of [6], where power law decay is always seen. Detailed considerations of the correspondence show that the results are broadly in agreement with these expectations, but modified by a variety of interesting extra features discussed below.

3. Null sector

We denote a sector whose IS contains no B elements as a null sector. In terms of the notation introduced earlier, this refers to $[0]^{\mathcal{L}}$ with $\mathcal{L} = N_C$ and $y = 1$. In any such sector, the DDRD with an even number of particles is isomorphic to directed diffusion of non-reconstituting or 'hard' dimers. The reason is that every cluster of ones must contain an even number of particles (otherwise the IS would not be all 0s), and hence a cluster can be labelled as $DEDEDEDE$, with a D at the start and E at the end. Each successive DE pair can be thought of as a dimer, which retains its identity forever: the elementary move $110 \to 011$ is $DE0 \to 0DE$. The problem of non-reconstituting hard dimers (and more generally k-mers) is of interest in several contexts, and some aspects have already been studied [10, 11]. This isomorphism allows us to obtain the correlation function for the reconstituting dimer problem, in the special case of the null sector, from the derivation given in section 5 for the non-reconstituting case.

We now summarize the results for the dynamic properties of interest in null sectors. A more detailed account will appear in [13]. By following the motion of a hole in the DDRD and its image in the ASEP we find that the ratio of the currents J_{DDRD} (for DDRD) and J_X is equal to the metric factor $L_X/L = 1/(1+x)$. Evidently, we then have $J_{\mathrm{DDRD}} = x(1-x)/(1+x)$.

3.1. Wheeling effect

An important effect shows up in a more detailed consideration of the mapping between sites in the ASEP and in the DDRD. A fixed site in the DDRD problem corresponds to a moving site in the ASEP—it wheels around the ring at a finite mean velocity. This happens because if we follow the ASEP image of a single jump $110 \to 011$ in the DDRD, we find that the image of the central site of the triplet advances by one unit, while the images of the other two sites remain unchanged. In time t, the displacement of a mapped site is thus $\Delta r(t) = Wt + \phi(t)$, where W is the wheeling velocity and $\phi(t)$ is a zero-mean variable which represents the effect of stochasticity in the motion. It can be shown [13] that in the null sector the wheeling velocity is given by

$$W = x(1-x)/(1+x). \tag{2}$$

The wheeling motion of ASEP sites has been verified by direct observation of mapped site motion in MC simulations, which shows a small jitter corresponding to $\phi(t)$ around the predicted average wheeling velocity.

3.2. Autocorrelation functions

The considerations of the previous paragraph have important consequences for the DDRD: correlation functions are like those of the ASEP only if wheeling of sites ($r \to r + Wt$) is allowed for. This suggests that in the long-time scaling regime, if the effects of jitter arising from the stochastic part $\phi(t)$ can be ignored, the density–density correlation function $C(r,t)$ of the DDRD in the null sector will be of the form

$$C(r,t) = t^{-2/3} F([r + (W-U)t]t^{-2/3}). \tag{3}$$

For the autocorrelation function ($r = 0$) the argument of F is proportional to the difference of the wheeling velocity and the kinematic wave speed U of the ASEP, $W - U = x(1 - x)/(1 + x) - (1 - 2x)$. Then, if F is similar to the scaling function g'' of the ASEP, the autocorrelation function $C(r = 0, t) \equiv C(t)$ of the null sector will decay as $t^{-2/3} \exp(-\kappa t)$ at large times, where κ is a constant proportional to $W - U$. On the other hand, in the special case where $W - U$ vanishes, late-time slower-than-exponential decay should be expected, that is $C(t) \propto t^{-2/3} Y(t)$ where Y falls slowly, e.g. approaching a constant. Notice that $W - U$ vanishes at the 'compensating' value x_c of the ASEP particle concentration given by

$$x_c = \sqrt{2} - 1, \tag{4}$$

which would correspond to an IS $[0]^{\mathcal{L}}$ of length $\mathcal{L} = L(\sqrt{2} - 1)$.

3.3. Numerical simulations

To support these expectations, we have conducted extensive simulations of forward-diffusing, reconstituting dimers in a variety of situations. Since autocorrelation functions of interest refer to spontaneous fluctuations in steady state (SS), we avoided the relaxation of the system by generating SS configurations directly, thus saving considerable CPU time. In the equivalent ASEP, all configurations in SS are equally weighted under periodic boundary conditions and can be translated to DDRD configurations. This enables us to average our measurements over a large number of samples to reduce scatter in the data.

In null sectors with IS of length $\mathcal{L}$, such initial conditions are obtained by random deposition of $(L - \mathcal{L})/2$ monomers on a ring of $(L + \mathcal{L})/2$ sites. Subsequently, each monomer is duplicated by adding another one over an extra adjacent location specially added for that purpose, i.e. $1 \to A = 11$, which leaves us with a ring of L sites and $(L - \mathcal{L})/2$ randomly distributed dimers. Notice that this generating procedure is not equivalent to a random sequential adsorption of dimers in the original system. Had the latter method been applied it would necessarily introduce correlations between dimers because of shielding effects among them [14, 15].

We then evolved our DDRD system using the stochastic microscopic rules referred to above. After a sequence of L update attempts at random locations, the timescale is increased by one unit, i.e. $t \to t + 1$, irrespective of these attempts being successful. Also, measurements at shorter (longer) time intervals can also be allowed by updating the system in $M < L$ ($M > L$) microsteps, and increasing t as $t + M/L$. Typically, we considered rings of 10^5 sites and averaged our measurements over 2×10^4 histories starting from the independent configurations constructed above. In figure 1 we show the resulting autocorrelation functions for various particle densities ρ in null sectors of length $\mathcal{L} = L(1 - \rho)$, or equivalently, at different concentrations $x = \rho/(2 - \rho)$ of the associated ASEP system. The full line corresponds to the compensating condition $x_c = \sqrt{2} - 1$, thus making $U - W = 0$, and is the case where slower-than-exponential decay is seen. Specifically, it is consistent with a large-time behaviour $C(t) \propto t^{-2/3}$, in turn suggesting that the slowly decaying function $Y(t)$ referred to after equation (3) approaches a constant at large t. This is in marked contrast to all other IS fractions studied which always give rise to exponential decays, either below or above x_c. This constitutes a strong confirmation of the theory.

In preparation for the analysis of SS currents in more general situations (see section 4), we also estimated these quantities numerically by measuring the three-point correlations involved in the assisted hopping, namely

$$J_1 = \frac{2}{L} \sum_i \langle n_{2i-1} n_{2i} \overline{n}_{2i+1} \rangle, \qquad J_2 = \frac{2}{L} \sum_i \langle n_{2i} n_{2i+1} \overline{n}_{2i+2} \rangle \tag{5}$$

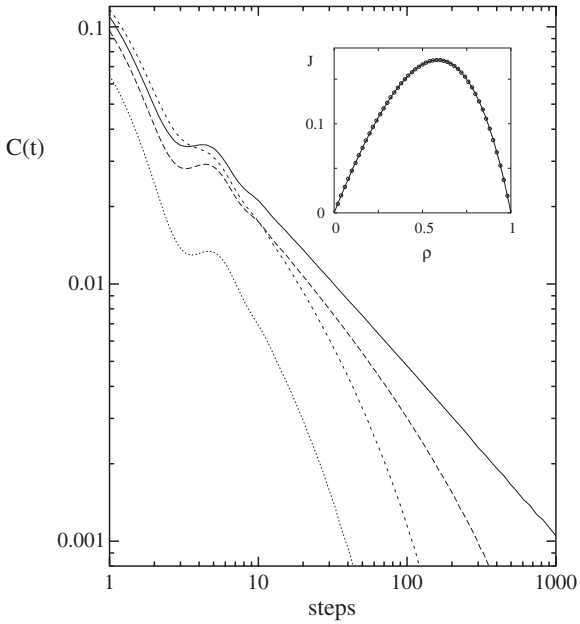

Figure 1. Autocorrelation functions of null strings $[0]^{\mathcal{L}}$ with different lengths $\mathcal{L}$. From bottom to top they refer to $\mathcal{L}/L = 1/5, 3/5, 1/3$ and $\sim\sqrt{2} - 1$ (compensating condition $W - U = 0$). The latter case is consistent with a $t^{-2/3}$ large-time decay, whereas the other situations give rise to exponential decays. The inset displays steady currents of null sectors with particle densities $\rho = 1 - \mathcal{L}/L$, closely following the analytical current $\rho(\rho - 1)/(\rho - 2)$ derived from section 3, and reaching a maximum near vanishing wave velocities.

on each of the sublattices 1 and 2, where $\overline{n} \equiv 1 - n$ denotes a vacancy. As will be discussed below, the compensating condition also corresponds to the vanishing of both current derivatives with respect to particle densities. The inset of figure 1 displays the currents of sector [0] (both equivalent in this case), as a function of the particle density ($\rho_1 = \rho_2$), closely following the J_{DDRD} current discussed above. As expected, its extremum occurs very near to $\rho_c = 2 - \sqrt{2}$, namely close to $x = x_c$.

3.4. DDRD and ASEP analogies

The above results would indicate that the long-time autocorrelations of the DDRD and ASEP systems are similar provided that the kinematic wave in each system is stationary. Despite the existence of jitter between site locations in the two systems, figure 2 provides a strong indication that this might be the case provided large times are considered ($t \gtrsim 20$). On the other hand, the short-time differences between both systems (see inset of figure 2) can be qualitatively understood by combining wheeling with the equal-time spatial structure, which, as will be discussed in section 5, has a finite SS correlation length. Moreover, analogues with the ASEP would suggest attempting a collapse of all the null sector DDRD autocorrelation data at $x \neq x_c$. Figure 3 shows the data collapse for the DDRD autocorrelation $C(t)$ at representative xs in the null sector, as a plot of $\ln[bt^{2/3}C(t)]$ versus at. There is a convincing collapse to a line corresponding to $\ln g''(s)$ versus s^3, where g'' is the ASEP scaling function (equation (1)) in which $s^3 \propto t$. As for a and b, they are fitting parameters which depend on x, and their numerical values [13] closely follow those arising from the analysis of [12, 16].

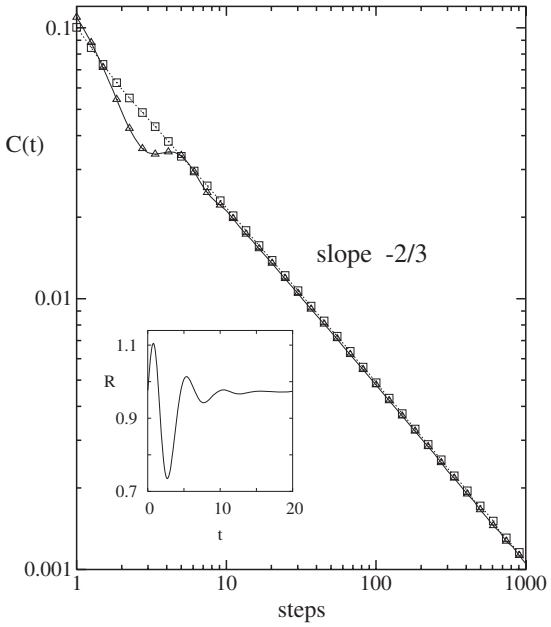

Figure 2. Comparison of ASEP (squares) and DDRD (triangles) autocorrelation functions at $x = 1/2$ and $x = x_c$, respectively (compensating conditions in both systems). Above ∼20 MC steps they both decay as $\sim t^{-2/3}$ and with very similar amplitudes. The short-time behaviour is shown by the inset displaying the ratio $R(t) = C_{\mathrm{DDRD}}(t)/C_X(t)$ which involves the wheeling effect referred to in section 3.

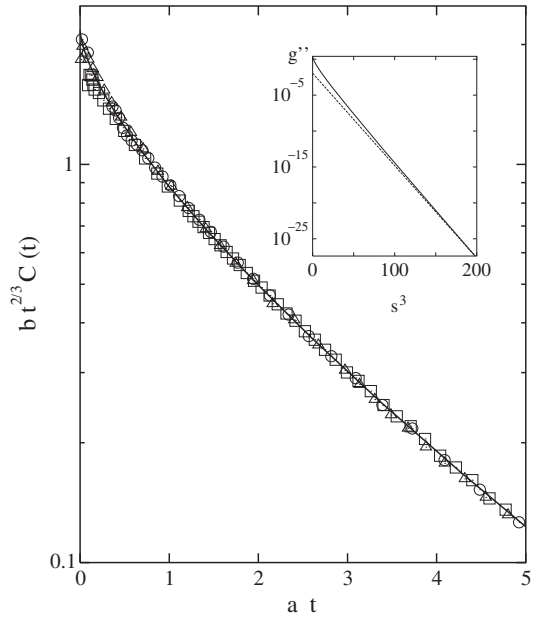

Figure 3. Data collapse of autocorrelations in sector $[0]^{\mathcal{L}}$ for non-critical regimes. They refer respectively to $\mathcal{L}/L = 3/5$ (squares), $1/5$ (circles) and $1/3$ (triangles). The curvature of the ASEP scaling function g'' (solid line, [12]) shows that the collapse achieved through the fitting parameters a, b is yet very far from the asymptote. The latter is only reached above $s^3 = at \gtrsim 200$, as hinted at by the actual behaviour of g'' exhibited in the inset. Nevertheless, the resulting values of a and b are understandable in terms of the analysis of g'' given in [12, 16] along with the wheeling velocity (equation (2)). For the purposes of display, all early time data ($at \lesssim 1/2$) have been pruned.

The argument s of $g''(s)$ and the overall prefactor required to give the autocorrelation function for the ASEP are given on dimensional grounds as functions of x in [12] and [16] (in particular, see equations (1.3)–(1.10) in [16]), and involve $U = (1 - 2x)$ and $J_X = x(1 - x)$ together with t in forms consistent with the scaling variables given in section 2. There are also numerical factors, which differ between the two papers. Our data collapse for the DDRD yields values for a which for most x are within 1% of the corresponding theoretical ASEP values [16]; likewise for b, except for a persistent difference of a factor of 2 (possibly owing to the definition

of g'' in [16]). Apart from this, the DDRD autocorrelations correspond in every detail to the ASEP ones except at early times.

The data in figure 3 do not lie in the asymptotic regime where $\ln g''(s)$ is linear in s^3. This exponential decay is achieved only for $s^3 \gtrsim 200$, as displayed in upper inset; the corresponding times are very large and the autocorrelations too small to render them numerically accessible by direct simulation. Size dependences are then noticeable unless $L^{3/2}$ is large compared to such times, so very large system sizes are required in the MC. Further, the implied large equilibration times mean that for large L it would not be feasible to prepare initial states by relaxation. In our simulations, initial states are obtained via the ASEP by exploiting its product measure property, as described above.

4. Periodic irreducible strings

In non-null sectors, the value of N_B is a measure of reconstitution that occurs in that sector. We have examined some sectors with periodic ISs and find pronounced oscillations in the autocorrelation functions, e.g. figures 4 and 5 correspond to sectors $[BCC]^{\mathcal{L}/3}$ ($y = 2/3$) and $[BBC]^{\mathcal{L}/3}$ ($y = 1/3$), with ISs composed of repeating units BCC and BBC, respectively. The time periods for such periodic sectors are readily calculated, since the oscillations are due to the alternations of ones and zeros arriving at a site.

4.1. Steady state construction

In this new scenario the initial steady configurations were prepared by means of a slight variation of the generating procedure described for null strings (section 3). Consider for instance the sector $[BCC]^{\mathcal{L}/3}$. Then, we can identify two types of 'single site holes' $B = 10$ and $C = 0$, within an ASEP ring of $L/2 + \mathcal{L}/4$ sites over which $(L - \mathcal{L})/2$ 'monomers' (later on recast as dimers $A = 11$), are randomly adsorbed. In going backwards from ASEP to DDRD, we first christen the ASEP vacancies as B or C, in the order in which they occur in the IS. While reconstructing the DDRD configuration, we expand out the Bs to be 10s and let the Cs be zeros. The resulting configuration is updated by our usual stochastic rules. This was carried out on DDRD rings of 1.2×10^5 sites and averaged typically over 3×10^4 independent histories. Particle densities, $\rho_2 = 1 - \frac{\mathcal{L}}{L}$ and $\rho_1 = 1 - \frac{\mathcal{L}}{2L}$, on even and odd sublattices, are preserved throughout $[x = (1 - \mathcal{L}/L)/(1 + \mathcal{L}/2L)]$, whereas both autocorrelations and currents were separately computed in each sublattice. A similar SS construction and numerical considerations apply to the $[BBC]^{\mathcal{L}/3}$ sector, with an evolution which now takes place in two equivalent sublattices of density $\rho = 1 - \frac{3\mathcal{L}}{5L}$ $[x = (1 - \mathcal{L}/L)/(1 + \mathcal{L}/5L)]$.

4.2. Sublattice currents and wave velocities

For sectors such as the above, with periodic ISs, a full discussion is possible for currents, compensating conditions and kinematic waves with velocities given by a density derivative of the appropriate current in the DDRD model. The compensating condition $W - U = 0$ then correspond to the vanishing of the kinematic wave velocity given by the current derivative in the DDRD process, at which point we expect slower-than-exponential decays of autocorrelations.

In these periodic sectors one can work out analytically the current on each sublattice using the DDRD–ASEP correspondence given in section 2, and hence obtain the critical x_c and the velocities (details can be found in [13]). If z_1 and $z_2 = 1 - z_1$ are the proportions of zeros on sublattices 1, 2, then the current associated with the movement of zeros on each sublattice is

$$J_i = 2xz_i(1 - x)/[2 - y(1 - x)], \qquad i = 1, 2. \tag{6}$$

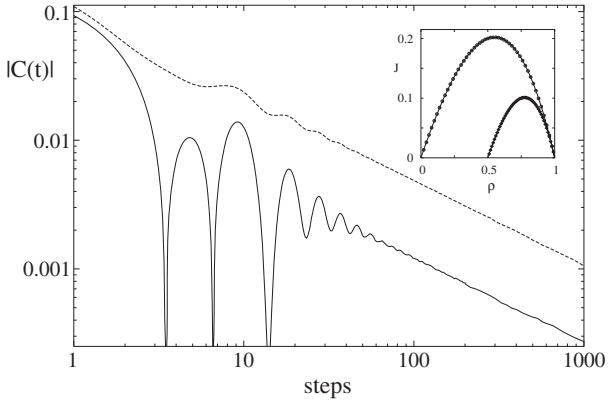

Figure 4. Autocorrelation functions of critical BCC sector ($\mathcal{L}_c/L \simeq \sqrt{6}-2$), for both even and odd sublattices (dashed and solid lines respectively). In both cases, the asymptotic behaviour is consistent with a $t^{-2/3}$ relaxation. As explained in the text, the early time oscillations are due to the periodicity of the four IS characters [1000]. The inset displays even and odd sublattice currents (upper and lower curves respectively), as functions of their corresponding densities $\rho_2 = 1 - \frac{\mathcal{L}}{L}$, $\rho_1 = 1 - \frac{\mathcal{L}}{2L}$. The data are accurately described by $J_2 = 2\rho_2(1-\rho_2)/(3-\rho_2)$ and $J_1 = (1-\rho_1)(2\rho_1-1)/(2-\rho_1)$, in agreement with equation (9). The critical condition of the main panel corresponds to maximum currents near $\rho_2 = 3-\sqrt{6}$, and $\rho_1 = 2-\sqrt{3/2}$, namely at vanishing wave velocities.

The corresponding DDRD sublattice kinematic wave velocities V_i are obtained from $V_i = \partial_{\rho_i} J_i$ where ρ_i are sublattice particle densities (of ones) in the DDRD. So V_1, V_2 vanish at a common value, x_c, of the ASEP density x given by $\partial_x[x(1-x)/(2-y(1-x))] = 0$. This is a quadratic equation for x, whose root lying between 0 and 1 is

$$x_c = [\sqrt{2(2-y)} - (2-y)]/y. \tag{7}$$

Thus, x_c is a monotonic decreasing function of y in the range $0 \leqslant y \leqslant 1$, varying between 0.5 and $\sqrt{2}-1$. As a check on the result for x_c, for the null sector we have $y = 1$, which implies $x_c = \sqrt{2}-1$.

It is easy to obtain the V_i from the J_i by relating the ρ_i to the particle density $\rho(x)$ in the full DDRD (from both sublattices), and thence to x (in terms of which we have J_i). The result is

$$V_i = 2 - 4x - y(1-x)^2, \tag{8}$$

independent of sublattice label i, implying that the two sublattice velocities are the same, as well as the x_c at which they vanish. For comparison with MC results (equation (5)), we can obtain similarly, in any sector with a periodic IS, the current on sublattice i of the DDRD in terms of the particle density ρ_i on sublattice i:

$$J_i = (1-\rho_i)[2z_i - (2-y)(1-\rho_i)]/[2z_i + y(1-\rho_i)]. \tag{9}$$

The analytical results for $[BCC]^{\mathcal{L}/3}$ and $[BBC]^{\mathcal{L}/3}$, obtained by inserting their respective y and z_i, are the full lines in the insets in figures 4 and 5, respectively (skewed parabolas as functions of sublattice densities). Like the null string currents discussed in section 3 (inset of figure 1), they agree closely with the data points resulting from the simulations. The sublattice autocorrelation functions shown in the corresponding main panels are at the densities of the maxima of the respective sublattice currents, and each show a $t^{-2/3}$ power law long-time decay, verifying in turn that they are at the critical density. Moreover, in analogy to null string cases,

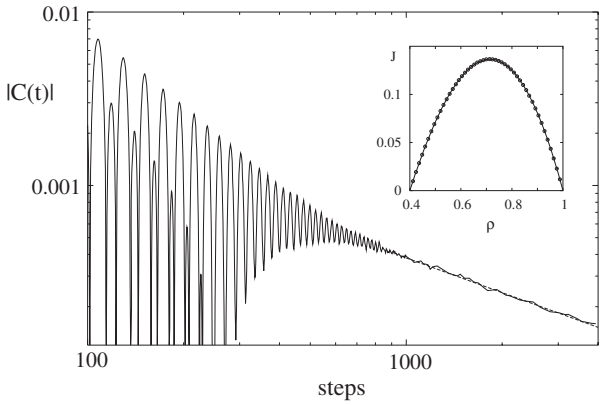

Figure 5. Autocorrelations of critical BBC string with length density $\mathcal{L}_c/L \simeq \sqrt{30} - 5$. The large-time behaviour follows closely a $t^{-2/3}$ power law decay (denoted by the rightmost lower dashed line). As in figure 4, the initial oscillations can be accounted for by the periodicity of the IS elements [10100]. The inset contains the steady currents (equivalent in both sublattices), which follow entirely their analytical counterparts $J = (\rho-1)(5\rho-2)/(\rho-4)$, in equation (9). The wave velocity vanishes at the current maximum, on approaching the main panel regime at $\rho = 4-3\sqrt{6/5}$.

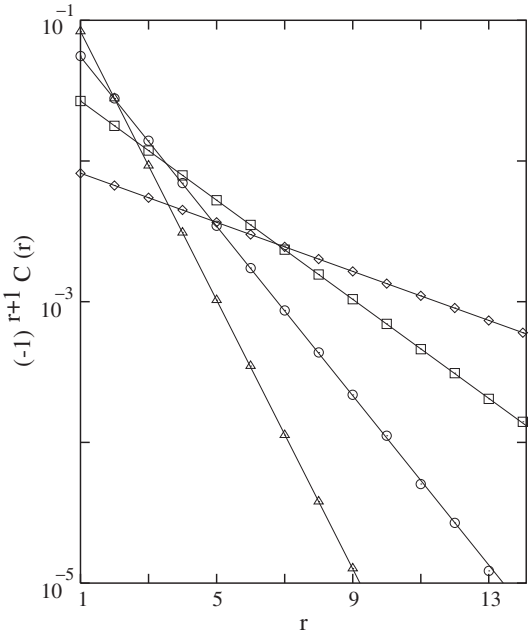

Figure 6. Spatial pair correlations of sector $[0]^{\mathcal{L}}$ for $\mathcal{L}/L = 1/2$ (triangles), $1/3$ (circles), $1/5$ (squares) and $1/10$ (rhomboids). The solid lines are fitted with slopes (inverse correlation length) $\xi^{-1} = \ln(\frac{1+\mathcal{L}/L}{1-\mathcal{L}/L})$, in agreement with equations (10) and (11). The actual oscillations of $C(r)$ also follow the behaviour predicted in section 5.

it was found that on departing from these critical conditions the observed power law decay changes abruptly to exponential.

5. Spatial correlations in null sectors

In the null sector $[0]^{\mathcal{L}=N_C}$ with an even number of particles the correlation function in the dimer problem can be evaluated exactly (below) using the isomorphism to non-reconstituting dimers together with the DE representation introduced in section 3. Since the presence of a D particle at site i implies and is implied by the presence of an E particle at site $(i+1)$, the (unsubtracted) particle–particle correlation function can be reduced to

$$\langle n(i)n(i+r)\rangle = 2\mathcal{E}(r) + \mathcal{E}(r-1) + \mathcal{E}(r+1), \tag{10}$$

where $\mathcal{E}(r)$ is the (unsubtracted) correlation function obtained from all configurations having an E particle at each of sites i and $i+r$. The weight of each such a configuration can be found by mapping it to the corresponding configuration in the equivalent ASEP. Allowing for the weights of the Es at i and $i+r$ and those of m dimers and $(r-2-2m)$ holes between, and for multiplicities, and summing over m (from 0 to the integer part of $(r-2)/2$) provides the required $\mathcal{E}(r)$. After reductions it becomes

$$\mathcal{E}(r) = [x^2/(1+x)^2][1-(-x)^{r-1}], \tag{11}$$

(for details, see [13]). Inserting into equation (10) above, and subtracting $\langle n\rangle^2 = [2x/(1+x)]^2$ provides the subtracted pair correlation function $C(r)$. This is oscillatory, and has a decaying envelope with correlation length $\xi = [\ln(1/x)]^{-1}$. Figure 6 shows MC results for the (subtracted) spatial correlations $C(r)$ in the null sector for various x. The actual $C(r)$s show the predicted oscillation $(-1)^r$, and the correlation lengths agree closely with the theory.

6. Concluding discussion

This investigation of the simplest model combining strongly broken ergodicity with driving has uncovered a wealth of properties, some expected and others not foreseen. In particular the model shows an interesting interplay between the collective (and scaling) kinetics of the basic driven model (the ASEP) and effects of the invariant IS which characterizes the sector in the DDRD. Monte Carlo simulations shows many of these features in striking fashion.

Despite the richness and complexity of the combined model, much has been understood analytically for sectors with null or periodic ISs. The scaling behaviour seen so far appears to be in the universality class of the ASEP. The relationships of non-universal variables, like currents, densities (including critical densities) and velocities, have been largely understood.

There are, however, certain important generalizations which have not been discussed here, which we now briefly mention: additional special sectors, alternative boundary conditions and k-mer generalizations.

We can expect, following the discussion of [6] for the DRD, new effects in sectors having ISs with various types of structural correlation. Provided critical conditions (x_cs) exist in which autocorrelations show power law time decay, the power law for such sectors need no longer be related simply to the ASEP exponents. One would then have different decay patterns, according to sector ('dynamic diversity'). The combination of the methods developed here with those of [6] might well allow analytical treatment of such effects.

Changing from periodic boundary conditions to open ones with boundary injection could strongly alter the behaviour. For the ASEP, that change produces non-trivial spatial correlations and dynamics and, most important of all, a steady state non-equilibrium phase transition. Density profiles, correlations and dynamics differ in the different phases. We would expect all these features to occur in the corresponding boundary-driven version of the DDRD, in cases like injection/ejection of dimers, so long as the injection and ejection processes keep the IS

intact. Again, the detailed properties would vary from sector to sector, and the methods used here should prove useful in this generalized situation.

Finally, generalizations from reconstituting dimers to k-mers, deserve consideration. As with dimers, the problem of non-reconstituting k-mers which is of current interest [10, 11] is contained in null sectors of the general problem. The sector-wise mapping to the ASEP still holds, but the number of sectors is much larger for larger k, as multiplicities in the types of ASEP holes increase with k. The sector-wise study of the dynamics remains to be explored systematically.

Acknowledgments

We are grateful to D Dhar, G Schütz, R Zia, C Godrèche, P Ferrari, H Spohn, S Majumdar, S Chatterjee, M Evans and M Moore for helpful observations and correspondence. MB's stay at the Newton Institute was supported through EPSRC grant 531174. MDG acknowledges support of CONICET, Argentina, under grants PIP 5037 and PICT ANCYPT 20350. The work of RBS was supported by EPSRC under the Oxford Condensed Matter Theory grants GR/R83712/01 and GR/M04426.

References

[1] Odor G 2004 *Rev. Mod. Phys.* **76** 663
[2] Barma M, Grynberg M D and Stinchcombe R B 1993 *Phys. Rev. Lett.* **70** 1033
[3] Stinchcombe R B, Grynberg M D and Barma M 1993 *Phys. Rev.* E **47** 4018
[4] Dhar D and Barma M 1993 *Pramana-J. Phys.* **41** L193
[5] Barma M and Dhar D 1994 *Phys. Rev. Lett.* **73** 2135
[6] Menon G I, Barma M and Dhar D 1997 *J. Stat. Phys.* **86** 1237
[7] Stinchcombe R B 2001 *Adv. Phys.* **50** 431
[8] Schütz G M 2001 *Phase Transitions and Critical Phenomena* vol 19, ed C Domb and J L Lebowitz (London: Academic)
[9] Lighthill M J and Whitham G B 1955 *Proc. R. Soc.* A **229** 281
[10] Shaw L B, Zia R K P and Lee K H 2003 *Phys. Rev.* E **68** 021910
[11] Schönherr G and Schütz G M 2004 *J. Phys. A: Math. Gen.* **37** 8215
[12] Prähofer M and Spohn H 2002 *In And Out of Equilibrium* (*Progress in Probability* vol 51) ed V Sidoravicius (Boston, MA: Birkhauser) pp 185–204 (*Preprint* cond-mat/0101200)
Tables of scaling functions are also given by Prähofer M and Spohn H 2002 http://www-m5.ma.tum.de/KPZ/
[13] Stinchcombe R B, Grynberg M D and Barma M in preparation
[14] Evans J W 1993 *Rev. Mod. Phys.* **65** 1281
[15] Grynberg M D 1996 *Annual Reviews of Computational Physics* vol 4, ed D Stauffer (Singapore: World Scientific) pp 185–240
[16] Ferrari P L and Spohn H 2006 *Commun. Math. Phys.* **265** 1